

MHD Flow and Heat Transfer through a Circular Cylinder Partially Filled with non-Darcy Porous Media

M. K. Sharma, Kuldip Singh, Ashok Kumar

Abstract- Steady incompressible axisymmetric flow in a circular cylinder partially filled with concentric cylinder of non-Darcy porous medium is studied in the influence of a transverse static magnetic field. The Joule heating effect produced by the magnetic field is also included to analyze effect of magnetic field and fluid flow field on heat convection process. The governing equations of flow and heat transfer are non-linear coupled differential equations, are solved with Quasi-numerical method – the Differential Transform method. The velocity and temperature profiles for the fluid saturated porous region and clear fluid annulus region are derived and computed with the use of Matlab at various physical parameters and there effects are discussed through graphs. The skin-friction coefficient and Nusselt number at the wall of the outer cylinder and at the surface of the concentric inner porous cylinder are computed and discussed.

Keywords: MHD, non-Darcy, Partial filled circular pipe, Joule heating.

Nomenclature:

K Permeability
 d Radius of the cylinder
 d_i Radius of porous cylindrical region
 \vec{q} Velocity of fluid flow
 \vec{J} Magnetic current density
 \vec{B} Applied magnetic field
 p Pressure
 G Constant pressure gradient
 T_f Fluid temperature in clear region
 T_p Fluid temperature in porous region
 Da Darcy number
 M Hartmann number
 Re Reynolds number
 F Forchheimer number
 u_f Fluid velocity in clear region
 u_p Fluid velocity in Porous region
 T_w Wall temperature

T_{pw} Temperature at surface of the porous cylinder

Greek symbols:

ρ Density of the fluid

μ Viscosity of the fluid

θ_p Non-dimensional fluid temperature in porous region

θ_f Non Dimensional fluid temperature in clear region.

I. INTRODUCTION

The flow through a semi porous medium is of great interest in oil refineries, chemical sciences, life sciences and medical sciences. In agriculture sector, the proper distribution of fertilizers and pesticides is insured using the cylindrical semi porous medium. The flow through semi porous cylindrical type configurations are encountered in many industries in one or other ways for cooling purposes or for heat connection processes. Loganathan et al. [7] studied MHD effects on free convective flow over moving semi-infinite vertical cylinder with temperature oscillation. Ziya Uddin et al. [12] studied heat and mass transfer characteristics and the flow behavior on MHD flow near the lower stagnation point of a porous isothermal horizontal circular cylinder. Chamkha A.J [4] investigated steady, laminar, hydromagnetic flow and heat and mass transfer over a permeable cylinder moving with a linear velocity in the presence of heat generation/absorption, chemical reaction, suction /injection effects developing a uniform transverse magnetic field. Abbas et al. [1] dealt with laminar flow and heat transfer of an electrically conducting viscous fluid over a stretching cylinder in the presence of thermal radiations through a porous medium. Nagaraju et al. [8] investigated the steady flow of an electrically conducting, incompressible micropolar fluid in a narrow gap between two concentric rotating vertical cylinders with porous lining on inside of outer cylinder under an imposed axial magnetic field. Yadav et al. [11] found out numerical solution of MHD fluid flow and heat transfer characteristics of a viscous incompressible fluid along a continuously stretching horizontal cylinder embedded in a porous medium in presence of internal heat generation or absorption. Aldoss [2] studied the MHD mixed convection flow about a vertical cylinder embedded in a non-Darcian porous medium with variable heat transfer boundary. Suneetha et al. [10] analyzed the interaction of free convection with thermal radiation of a viscous incompressible unsteady.

Manuscript published on 30 December 2014.

*Correspondence Author(s)

M. K. Sharma, Department of Mathematics, Guru Jambheshwar University of Science & Technology, Hisar.

Kuldip Singh, Department of Mathematics, Guru Jambheshwar University of Science & Technology, Hisar.

Ashok Kumar, Department of Mathematics, Guru Jambheshwar University of Science & Technology, Hisar.

© The Authors. Published by Blue Eyes Intelligence Engineering and Sciences Publication (BEIESP). This is an open access article under the CC-BY-NC-ND license <http://creativecommons.org/licenses/by-nc-nd/4.0/>

MHD flow past a moving vertical cylinder with heat and mass transfer in a porous medium. Shihhao et al. [9] derived analytical solution for MHD flow of a magnetic fluid within a thick porous annulus. In present study, the effect of magnetic field and Joule heating in the flow and heat transfer in a circular tube having a concentric circular porous cylinder of non-Darcy behavior are investigated.

II. FORMULATION OF THE PROBLEM

Steady incompressible non-Darcy, axisymmetric flow of electrically conducting fluid through a partially filled circular cylinder is considered. The porous material cylinder of radius c_i is concentric with the outer cylinder of radius d ($c_i < d$). In the cylindrical coordinates (r, θ, z) the axis of cylinder coincides with the z -axis. A static magnetic field of strength $(B_0, 0, 0)$ is applied on the cylinder. Thus the flow in $0 \leq r \leq c_i$ is non-Darcy flow and in the region $c_i \leq r \leq d$, flow of the fluid with annulus.

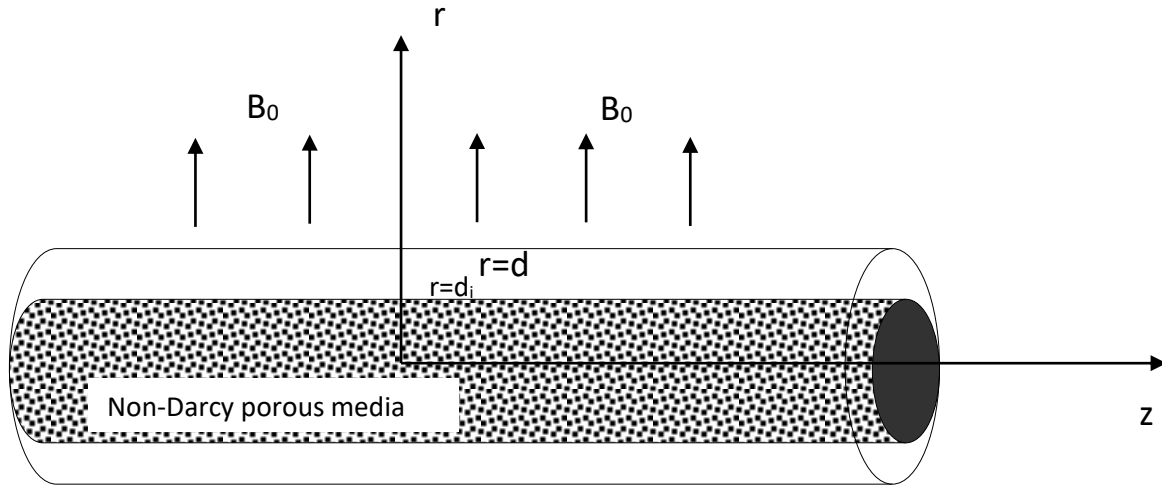


Figure 1 Physical model of the problem

The equation of continuity is defined as

$$\nabla \cdot \vec{q} = 0 \quad \dots (1)$$

The equations of motion are

$$\rho(\vec{q} \cdot \nabla \vec{q}) = -\nabla p + \mu \nabla^2 \vec{q} - \frac{\mu}{K} \vec{q} - \frac{\mu c_d}{\sqrt{K}} |\vec{q}| \vec{q} + \vec{J} \times \vec{B} \quad \dots (2)$$

The equation of energy

$$\rho c_p (\vec{q} \cdot \nabla T) = \nabla^2 T + \frac{\vec{J}^2}{\sigma} \quad \dots (3)$$

Under the above assumptions the equations of motion and energy for the annulus fluid region $c_i \leq r \leq d$ are given by

$$\mu \left(\frac{\partial^2 u_f}{\partial r^2} + \frac{1}{r} \frac{\partial u_f}{\partial r} \right) - \frac{\partial p}{\partial x} - \sigma B_0^2 u_f = 0 \quad \dots (4)$$

$$\kappa \left(\frac{\partial^2 T_f}{\partial r^2} + \frac{1}{r} \frac{\partial T_f}{\partial r} \right) + \sigma B_0^2 u_f^2 = 0 \quad \dots (5)$$

The equation of motion and energy for the porous region $0 \leq r \leq c_i$ are given by

$$\mu \left(\frac{\partial^2 u_p}{\partial r^2} + \frac{1}{r} \frac{\partial u_p}{\partial r} \right) - \frac{\partial p}{\partial x} - \sigma B_0^2 u_p - \frac{\mu}{K} u_p - \frac{\mu c_d}{\sqrt{K}} u_p^2 = 0 \quad \dots (6)$$

$$\kappa \left(\frac{\partial^2 T_p}{\partial r^2} + \frac{1}{r} \frac{\partial T_p}{\partial r} \right) + \sigma B_0^2 u_p^2 = 0 \quad \dots (7)$$

The corresponding boundary conditions are

$$\begin{aligned} r = 0 : \quad & \frac{\partial u_p}{\partial r} = 0, \quad \frac{\partial T_p}{\partial r} = 0 \\ r = d : \quad & u_f = 0, \quad T_f = T_w \end{aligned} \quad \dots (8)$$

$$r = d_i : \quad u_f = u_p, \quad T_f = T_p$$

$$\dots (9)$$

Where K permeability, u_f and T_f the velocity and temperature of the fluid in the annulus region, u_p and T_p the velocity and temperature of the fluid in the porous region, T_w temperature of the wall of cylinder, T_{pw}

temperature at the surface of porous cylinder, μ viscosity of the fluid σ electrical conductivity, C_d drag-force constant.

III. METHOD OF SOLUTION

To make the differential equations (4) to (7) dimensionless, introducing the following non-dimensional quantities

$$r^* = \frac{r}{d}, \quad x^* = \frac{x}{d}, \quad di^* = \frac{d_i}{d}, \quad u_f^* = \frac{u_f}{V_0}, \quad u_p^* = \frac{u_p}{V_0}, \quad G^* = \frac{\partial p}{\partial x} / \frac{\rho V_0^2}{d}, \quad Re = \frac{\rho V_0 d}{\mu},$$

$$M = \sqrt{\frac{\sigma B_0^2 d^2}{\mu}}, \quad Da = \frac{\mu}{K}, \quad F = \frac{c_d G d^4}{\sqrt{K} \nu \mu}, \quad \theta_f = \frac{T_f - T_w}{T_{pw} - T_w}, \quad \theta_p = \frac{T_p - T_w}{T_{pw} - T_w}, \quad Br = \frac{G^2 di^4}{\mu \kappa (T_w - T_{pw})} \quad \text{Where}$$

G the constant dimensionless pressure gradient, Da the Darcy number, Re the Reynolds number, M the Hartmann number, F the Forchheimer number, Br the Brinkman number. There is no loss of generality if the asterisks are dropped from the dimensionless form of the equations (4) to (7) the respective equations are given by

$$\frac{d^2 u_f}{dr^2} + \frac{1}{r} \frac{du_f}{dr} = ReG + M^2 u_f$$

$$\dots (10)$$

$$\frac{d^2 \theta_f}{dr^2} + \frac{1}{r} \frac{d\theta_f}{dr} + M^2 Br u_f^2 = 0$$

$$\dots (11)$$

$$\frac{d^2 u_p}{dr^2} + \frac{1}{r} \frac{du_p}{dr} = ReG + \left(\frac{1}{Da} + M^2 \right) u_p + \frac{F}{Re} u_p^2$$

$$\dots (12)$$

$$\frac{d^2 \theta_p}{dr^2} + \frac{1}{r} \frac{d\theta_p}{dr} + M^2 Br u_p^2 = 0$$

$$\dots (13)$$

The corresponding boundary conditions are

$$r = 0 : \quad \frac{\partial u_p}{\partial r} = 0 \quad \frac{\partial \theta_p}{\partial r} = 0$$

$$r = 1 : \quad u_f = 0 \quad \theta_f = 0$$

$$\dots (14)$$

At the interface

$$r = di : \quad u_f = u_p, \quad \theta_f = \theta_p \quad \dots (15)$$

Solution of the coupled momentum and energy equations, are obtained by the Differential Transform Method (DTM). The efficiency of method can be seen in literature [3], [5], [6].

The differential transform $U(k)$ of the derivative

$$\frac{d^k u(y)}{dy^k} \quad \text{is defined by} \quad U(k) = \frac{1}{k!} \left[\frac{d^k u(y)}{dy^k} \right]_{y=y_0}$$

The inverse differential transform of $U(k)$ is defined by

$$u(y) = \sum_{k=0}^{\infty} U(k) (y - y_0)^k$$

Table1: The fundamental mathematical operations under DTM

Function	Differential transform
$u(y) = f(y) \pm g(y)$	$U(k) = F(k) \pm G(k)$
$u(y) = \lambda g(y)$	$U(k) = \lambda G(k)$
$u(y) = \frac{\partial g(y)}{\partial y}$	$U(k) = (k+1)G(k+1)$
$u(y) = \frac{\partial^m g(y)}{\partial y^m}$	$U(k) = (k+1) \dots (k+m)G(k+m)$

$u(y) = y^m$	$U(k) = \delta(k - m) = \begin{cases} 1 & \text{at } k = m \\ 0 & \text{otherwise} \end{cases}$
$u(y) = f(y)g(y)$	$U(k) = \sum_{r=0}^k F(r)G(k-r)$
$u(y) = f_1(y)f_2(y)\dots f_m(y)$	$U(k) = \sum_{k_1}^k \dots \sum_{k_{m-1}=0}^{k_2} F_1(k_1)F_2(k_2 - k_1)\dots F_m(k - k_{m-1})$

3.1 Calculation for the velocity profiles

3.1.1 Velocity profile in annulus region

Applying DTM on (10) we will get the following recurrence relation

$$\sum_{h=0}^k \delta(h-1) \left((k-h+1)(k-h+2)U_f(k-h+2) + (k+1)U_f(k+1) \right) = GRe \delta(k-1) + M^2 \sum_{h=0}^k \delta(h-1)U_f(k-h) \dots (16)$$

Where $U_f(k)$ is differential transform of $u_f(r)$. Since the value of $u_f(r)$ at $r=0$ is not known explicitly, therefore assuming $U_f(0) = a$ (constant) which will be determined later with the prescribed boundary conditions.

For $k=0, 1, 2, 3, 4, 5$ in (16) we get

$$U_f(1) = 0, \quad U_f(2) = \frac{1}{4}(GRe + M^2 a), \quad U_f(3) = 0, \\ U_f(4) = \frac{M^2}{64}(GRe + M^2 a), \quad U_f(5) = 0, \quad U_f(6) = \frac{M^4}{2304}(GRe + M^2 a)$$

Using the above values in the inverse differential transform of $U_f(k)$ the velocity profile is given by

$$u_f(r) = a + \frac{1}{2^2}(GRe + M^2 a)r^2 + \frac{M^2}{2^2 4^2}(GRe + M^2 a)r^4 + \frac{M^4}{2^2 4^2 6^2}(GRe + M^2 a)r^6 \dots (17)$$

Using the boundary condition at $r = 1$, the arbitrary constant 'a' is obtained and given by

$$a = - \frac{\left(\frac{1}{4} + \frac{M^2}{64} + \frac{M^4}{2304} \right) GRe}{\left(1 + \frac{M^2}{4} + \frac{M^4}{64} + \frac{M^6}{2304} \right)}$$

Using value of 'a' in the equation (17), we get the velocity profile of the fluid in the annulus region.

3.1.2 Velocity profile in porous region

Applying DTM on (12), we get the recurrence relation

$$\sum_{h=0}^k \delta(h-1) \left((k-h+1)(k-h+2) U_p(k-h+2) + (k+1) U_p(k+1) \right) \\ = G \operatorname{Re} \delta(k-1) + \left(\frac{1}{Da} + M^2 \right) \sum_{h=0}^k \delta(h-1) U_p(k-h) + \frac{F}{\operatorname{Re}} \sum_{h=0}^k \sum_{i=0}^h \delta(i-1) U_p(h-i) U_p(k-h) \\ \dots(18)$$

where, $U_p(k)$ is differential transform of $u_p(r)$. Since value of $u_p(r)$ is not known at $r=0$ explicitly therefore assuming $U_p(0)=b$ (constant), which will be determined later with the aid of interface conditions.

Corresponding to $k=0, 1, 2, 3, 4, 5$ the recurrence relation (18) gives

$$U_p(1)=0, \quad U_p(2)=\frac{1}{2^2} \left(\operatorname{Re} G + \left(\frac{1}{Da} + M^2 \right) b + \frac{F}{\operatorname{Re}} b^2 \right), \quad U_p(3)=0,$$

$$U_p(4)=\frac{1}{2^2 4^2} \left(\frac{1}{Da} + M^2 + 2 \frac{F}{\operatorname{Re}} b \right) \left(\operatorname{Re} G + \left(\frac{1}{Da} + M^2 \right) b + \frac{F}{\operatorname{Re}} b^2 \right), \quad U_p(5)=0,$$

$$U_p(6)=\frac{1}{2^2 4^2 6^2} \left(\frac{1}{Da} + M^2 + 2 \frac{F}{\operatorname{Re}} b \right)^2 \left(\operatorname{Re} G + \left(\frac{1}{Da} + M^2 \right) b + \frac{F}{\operatorname{Re}} b^2 \right) \\ + \frac{1}{4^2 6^2} \left(\operatorname{Re} G + \left(\frac{1}{Da} + M^2 \right) b + \frac{F}{\operatorname{Re}} b^2 \right)^2$$

Using these values in the inversion of $U_p(k)$, we have

$$u_p(r) = b + \frac{1}{2^2} \left(\operatorname{Re} G + \left(\frac{1}{Da} + M^2 \right) b + \frac{F}{\operatorname{Re}} b^2 \right) r^2 \\ + \frac{1}{2^2 4^2} \left(\frac{1}{Da} + M^2 + 2 \frac{F}{\operatorname{Re}} b \right) \left(\operatorname{Re} G + \left(\frac{1}{Da} + M^2 \right) b + \frac{F}{\operatorname{Re}} b^2 \right) r^4 \\ + \left(\frac{1}{2^2 4^2 6^2} \left(\frac{1}{Da} + M^2 + 2 \frac{F}{\operatorname{Re}} b \right)^2 \left(\operatorname{Re} G + \left(\frac{1}{Da} + M^2 \right) b + \frac{F}{\operatorname{Re}} b^2 \right) \right. \\ \left. + \frac{1}{4^2 6^2} \left(\operatorname{Re} G + \left(\frac{1}{Da} + M^2 \right) b + \frac{F}{\operatorname{Re}} b^2 \right)^2 \right) r^6 \dots(19)$$

Now the interface condition provides that

$$\begin{aligned}
 a + \left(\frac{1}{2^2} di^2 + \frac{M^2}{2^2 4^2} di^4 + \frac{M^4}{2^2 4^2 6^2} di^6 \right) \left(G \text{Re} + M^2 a \right) &= b + \frac{1}{2^2} \left(\text{Re}G + \left(\frac{1}{Da} + M^2 \right) b + \frac{F}{\text{Re}} b^2 \right) di^2 \\
 &+ \frac{1}{2^2 4^2} \left(\frac{1}{Da} + M^2 + 2 \frac{F}{\text{Re}} b \right) \left(\text{Re}G + \left(\frac{1}{Da} + M^2 \right) b + \frac{F}{\text{Re}} b^2 \right) di^4 \\
 &+ \left(\frac{1}{2^2 4^2 6^2} \left(\frac{1}{Da} + M^2 + 2 \frac{F}{\text{Re}} b \right)^2 \left(\text{Re}G + \left(\frac{1}{Da} + M^2 \right) b + \frac{F}{\text{Re}} b^2 \right) \right. \\
 &\quad \left. + \frac{1}{4^2 6^2} \left(\text{Re}G + \left(\frac{1}{Da} + M^2 \right) b + \frac{F}{\text{Re}} b^2 \right)^2 \right) di^6 \\
 &\dots (20)
 \end{aligned}$$

Now (20) is a polynomial of 4th degree in b. A Matlab code has been generated for the computation of unknown constant b and using this value, the velocity profile in the porous region is known, computed and presented through graphs.

3.2 Calculation for Temperature profiles

3.2.1 Temperature profile in annulus region

Applying DTM on (11), we get recurrence relation

$$\begin{aligned}
 \sum_{h=0}^k \delta(h-1) (k-h+1) (k-h+2) \Theta_f(k-h+2) + (k+1) \Theta_f(k+1) &= \\
 -M^2 Br \sum_{h=0}^k \sum_{i=0}^h \delta(i-1) U_f(h-i) U_f(k-h) & \\
 \dots (21) &
 \end{aligned}$$

Where $\Theta_f(k)$ is differential transform of $\theta_f(r)$

Let $\Theta_f(0) = c$ (constant) will be determined with the aid of boundary condition on $\theta_f(r)$

Corresponding to $k=0, 1, 2, 3, 4, 5, 6, 7$ the recurrence relation (21) gives

$$\Theta_f(1) = 0, \quad \Theta_f(2) = -\frac{M^2 Br}{4} a^2,$$

$$\Theta_f(3) = 0,$$

$$\Theta_f(4) = -\frac{M^2 Br}{8} U_f(2),$$

$$\Theta_f(5) = 0$$

$$\Theta_f(6) = -\frac{M^2 Br}{36} (2a U_f(4) + U_f(2)^2)$$

$$\Theta_f(7) = 0$$

$$\Theta_f(8) = -\frac{M^2 Br}{32} (a U_f(6) + U_f(2) U_f(4))$$

Using these values in the inversion of differential transform of $\Theta_f(k)$ we have

$$\theta_f(r) = c + \Theta_f(2) r^2 + \Theta_f(4) r^4 + \Theta_f(6) r^6 + \Theta_f(8) r^8$$

With the use of boundary condition $\theta_f(1) = 0$, the constant c is determined and given by

$$c = -\Theta_f(2) - \Theta_f(4) - \Theta_f(6) - \Theta_f(8)$$

Furthermore, the temperature profile in the annulus region is given by

$$\begin{aligned} \theta_f(r) = & \frac{M^2 Br a^2}{4} (1-r^2) + \frac{M^2 Br}{32} (GRe + aM^2) (1-r^4) \\ & + \frac{M^2 Br}{36} \left(\frac{aM^2}{32} (GRe + aM^2) + \frac{1}{16} (GRe + aM^2) \right) (1-r^6) \\ & - \frac{M^2 Br}{32} \left(a \left(\frac{M^4}{2304} (GRe + M^2 a) \right) + \frac{M^2}{625} (GRe + M^2 a)^2 \right) r^8 \end{aligned}$$

3.2.2 Temperature profile for porous region:

Applying DTM on (13), we get recurrence relation

$$\begin{aligned} \sum_{h=0}^k \delta(h-1)(k-h+1)(k-h+2)\Theta_p(k-h+2) + (k+1)\Theta_p(k+1) \\ = -M^2 Br \sum_{h=0}^k \sum_{i=0}^h \delta(i-1)U_p(h-i)U_p(k-h) \end{aligned}$$

... (23)

Where $\Theta_p(k)$ is differential transform of $\theta_p(r)$. Since the initial value $\Theta_p(0)$ is not known, therefore assuming its differential transform $\Theta_p(0) = \alpha$ (constant) will be determined from interface condition.

Corresponding to $k=0, 1, 2, 3, 4, 5$ the recurrence relation (23) gives

$$\Theta_p(1) = 0$$

$$\Theta_p(2) = -\frac{M^2 Br}{4} a^2$$

$$\Theta_p(3) = 0$$

$$\Theta_p(4) = -\frac{M^2 Br}{8} U_p(2)$$

$$\alpha = c + (\Theta_f(2) - \Theta_p(2))di^2 + (\Theta_f(4) - \Theta_p(4))di^4 + (\Theta_f(6) - \Theta_p(6))di^6 + (\Theta_f(8) - \Theta_p(8))di^8 \quad \dots (25)$$

Invoking value of c in (25), the temperature profiles for porous region is computed from (24) with help of Matlab programming and presented through graphs.

IV. SKIN FRICTION COEFFICIENT

The non-dimensional shearing stress at the wall of the circular pipe and at the surface of porous cylinder in terms of the local skin-friction coefficient is derived as follows and computed values are given in table 2 & 3.

$$\Theta_p(5) = 0$$

$$\Theta_p(6) = -\frac{M^2 Br}{36} (2aU_p(4) + U_p^2(2))$$

$$\Theta_p(8) = -\frac{M^2 Br}{32} (bU_p(4) + U_p(2)U_p(4))$$

$$\theta_p(r) = \alpha + \Theta_p(2)r^2 + \Theta_p(4)r^4 + \Theta_p(6)r^6 + \Theta_p(8)r^8$$

... (24)

On applying the interface condition the equation (24), gives the value of unknown constant α .

$$C_f = \left(\frac{\mu}{\rho V_0^2} \frac{\partial u}{\partial r} \right)_{r=d}$$

The skin friction at the wall of the pipe

$$C_f = \frac{1}{\text{Re}} \left(\frac{\partial u_f}{\partial r} \right)_{r=1}$$

The skin friction at the surface of the porous cylinder

$$C_f = \frac{1}{\text{Re}} \left(\frac{\partial u_p}{\partial r} \right)_{r=di}$$

V. NUSSELT NUMBER

The non-dimensional coefficient of heat transfer at the wall of the circular pipe and at the surface interface of the porous cylinder is derived as follows and computed values are given in table 4 & 5.

Nusselt number at the wall of the pipe

$$Nu = - \left(\frac{\partial \theta_f}{\partial r} \right)_{r=1}$$

Nusselt number at the surface of the porous cylinder

$$Nu = - \left(\frac{\partial \theta_p}{\partial r} \right)_{r=di}$$

VI. RESULTS AND DISCUSSION

The flow profiles in figure 2 explore the effect of magnetic field on fluid velocity. It is depicted that flow velocity retarded due to Lorenzian force in both the region, in the core porous region and in the annulus region. The presence of fluid in the annulus region surrounding the porous cylinder dragging the fluid flowing in the core cylinder in the vicinity of the surface, results of which there is a large velocity gradient at the surface of the core cylinder and hence the shear stress. When strength of the transverse magnetic field is increased the velocity gradient at the interface has been diminishes, consequently the shear stress at the surface. The effect of Reynolds number is shown in the figure 3. Which demonstrates that the increase in Reynolds number enhance the fluid velocity in core region of non-Darcy porous media and also in the annulus region of the clear fluid. Furthermore it is plausible that the velocity gradient at the interface increases with the increase of Reynolds number. The Forchheimer number also controlling

significantly the velocity gradient in the core region of non-Darcy porous media as observed from figure 4. The increase in Forchheimer number supports in the increase of the velocity of fluid in forward direction in the core region and reduces the velocity gradient in the vicinity of the circumference of this cylinder. The figure 5 demonstrates that the increase of Darcy number support in advancing the fluid velocity in the core region and reduces the velocity gradient in the peripheral region of the porous cylinder. Figure 6 depicts that the increase in pressure gradient in the flow direction enhances the fluid velocity in the flow direction in both, the core as well as in the annulus region. The mathematical results also endorse the physical concept related to flow and pressure gradient. The temperature of the fluid in the saturated porous medium in the core region and also the temperature of the fluid in annulus region increases at small values of Hartmann number up to 2 as observed in the figure 7. The increase in Reynolds number, pressure gradient and the Brinkman number increases the temperature of the fluid in the saturated porous medium in the core region and also the temperature of the fluid in annulus region are shown in the figure 8, figure 11 and figure 12, respectively. The temperature of the fluid in core region decreases with the increase in Forchheimer number while increases with the increase in Darcy number are shown in the figure 9 and figure 10, respectively. Table 2 and 3 depicts that the shear stress increases at the wall of cylinder but decreases at surface of porous cylinder with increase in Hartmann number while The Darcy number and pressure gradient have converse effect on skin effect to Hartmann number. In table 4 and 5, heat convection increases for small values of Hartmann number up to 2 and then decreases both at porous cylinder and wall of the annulus. Increase in Reynolds number and Brinkman enhances the heat convection both at annulus wall and porous surface.

VII. CONCLUSIONS

- The magnetic field is acting as shear controlling device as with the increase in Hartmann number the shear stress at the surface of the core cylinder is reduced.
- The Forchheimer number also significantly controlling the velocity gradient in the core region
- The heat convection enhanced with the increase in Brinkman number and Reynolds number.
- The heat convection decrease with the increase in Darcy number at the surface of porous cylinder.

Table 2. Skin friction at the wall of outer cylinder

M	Re	F	Da	G	Cr
1	10	5	0.1	-10	-4.46349
1.5	10	5	0.1	-10	-3.97079
2	10	5	0.1	-10	-3.47561
3	10	5	0.1	-10	-2.635408



3	20	5	0.1	-10	-2.6354085
3	30	5	0.1	-10	-2.63540833
3	40	5	0.1	-10	-2.63540825
3	10	1	0.1	-10	-2.635408
3	10	10	0.1	-10	-2.635408
3	10	15	0.1	-10	-2.635408
3	10	5	1	-10	-2.635408
3	10	5	0.01	-10	-2.635408
3	10	5	0.1	-1	-0.263541
3	10	5	0.1	-15	-3.953112
3	10	5	0.1	-20	-5.270817

Table 3. Skin friction at the surface of porous cylinder

M	Re	F	Da	G	C _f
1	10	5	0.1	-10	2.660946
1.5	10	5	0.1	-10	2.016756
2	10	5	0.1	-10	1.465833
3	10	5	0.1	-10	0.780006
3	20	5	0.1	-10	0.7800055
3	30	5	0.1	-10	0.78000567
3	40	5	0.1	-10	0.78000575
3	10	1	0.1	-10	0.633271
3	10	10	0.1	-10	0.974529
3	10	15	0.1	-10	1.155216
3	10	5	1	-10	0.985417
3	10	5	0.01	-10	2.91818
3	10	5	0.1	-1	0.061627
3	10	5	0.1	-15	1.31669
3	10	5	0.1	-20	1.949058

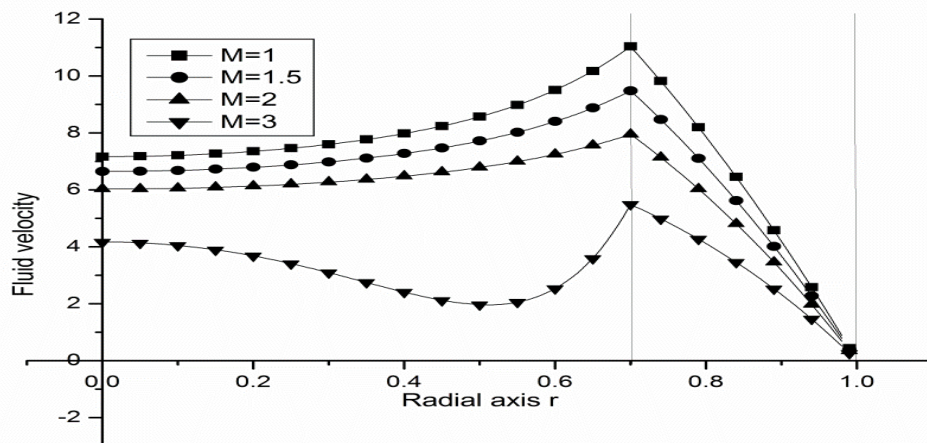
Table 4. Nusselt number at wall of the outer cylinder

M	Re	F	Da	G	Br	Nu
1	10	5	0.1	-10	0.01	0.69669
1.5	10	5	0.1	-10	0.01	1.03043
2	10	5	0.1	-10	0.01	1.14515
3	10	5	0.1	-10	0.01	1.07469
5	10	5	0.1	-10	0.01	0.85407
8	10	5	0.1	-10	0.01	0.5409
3	20	5	0.1	-10	0.01	4.29874
3	30	5	0.1	-10	0.01	9.67217
3	40	5	0.1	-10	0.01	17.19496
3	10	1	0.1	-10	0.01	1.07469
3	10	10	0.1	-10	0.01	1.07469
3	10	15	0.1	-10	0.01	1.07469
3	10	5	1	-10	0.01	1.07469
3	10	5	0.01	-10	0.01	1.07469
3	10	5	0.1	-15	0.01	2.41804
3	10	5	0.1	-20	0.01	4.29874
3	10	5	0.1	-10	0.05	5.37343
3	10	5	0.1	-10	0.1	10.74685

3	10	5	0.1	-10	0.2	21.4937
---	----	---	-----	-----	-----	---------

Table 5. Nusselt number at the surface of porous cylinder

M	Re	F	Da	G	Br	Nu
1	10	5	0.1	-10	0.01	0.24738
1.5	10	5	0.1	-10	0.01	0.45732
2	10	5	0.1	-10	0.01	1.64674
3	10	5	0.1	-10	0.01	0.80107
5	10	5	0.1	-10	0.01	0.66965
8	10	5	0.1	-10	0.01	0.38641
3	20	5	0.1	-10	0.01	3.20427
3	30	5	0.1	-10	0.01	7.20961
3	40	5	0.1	-10	0.01	12.81709
3	10	1	0.1	-10	0.01	0.88753
3	10	10	0.1	-10	0.01	0.7094
3	10	15	0.1	-10	0.01	0.63506
3	10	5	1	-10	0.01	0.9844
3	10	5	0.01	-10	0.01	0.10759
3	10	5	0.1	-15	0.01	1.69417
3	10	5	0.1	-20	0.01	2.83758
3	10	5	0.1	-10	0.05	4.00534
3	10	5	0.1	-10	0.1	8.01068
3	10	5	0.1	-10	0.2	16.02136


Figure 2. The effect of Hartmann number on fluid flow profile at $Re=10$, $F=5$, $Da=0.1$, $G=-10$

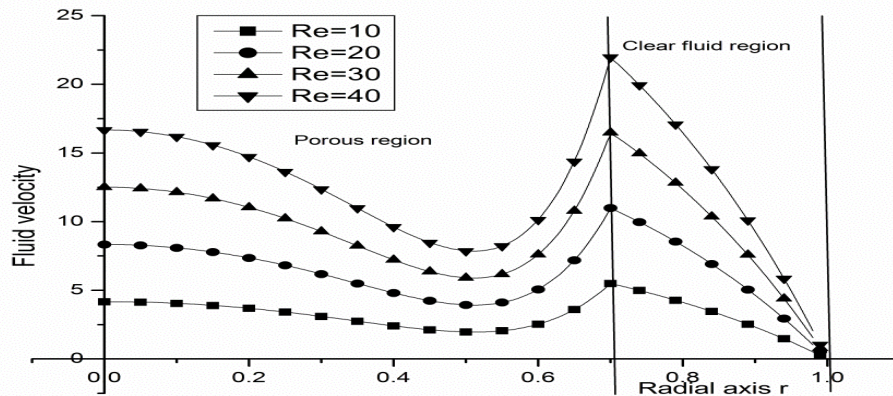


Figure 3. Effect of Reynolds number on fluid flow profile at $M=3$, $F=5$, $Da=0.1$, $G=-10$

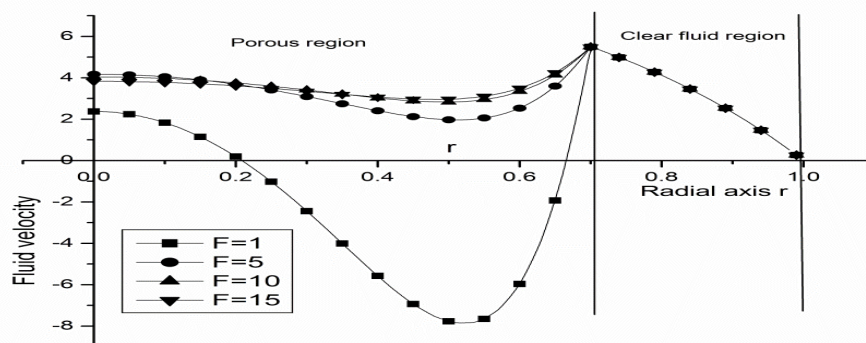


Figure 4. Effect of Forchheimer number on fluid flow profile at $M=3$, $Re=10$, $Da=0.1$, $G=-10$

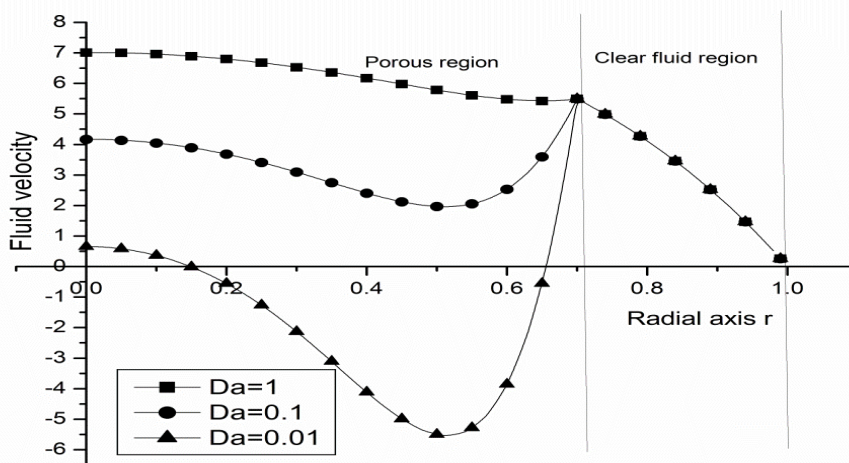


Figure 5. Effect of Darcy number on fluid flow profile at $M=3$, $Re=10$, $F=5$, $G=-10$

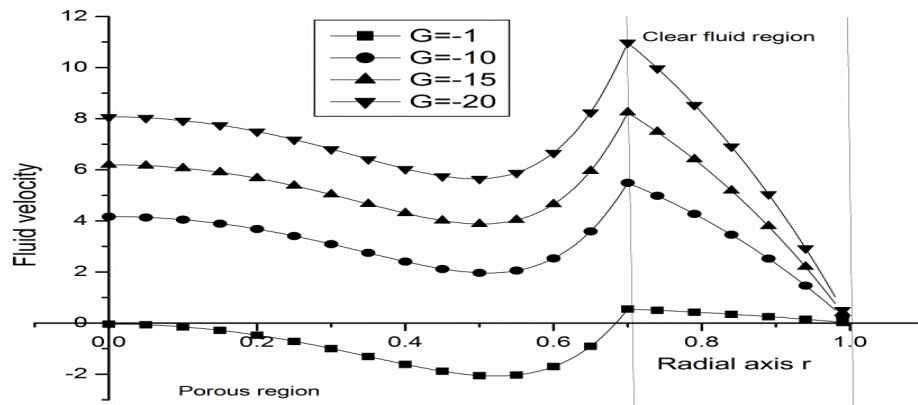


Figure 6. Effect of pressure gradient on fluid velocity profile at $M=3$, $Re=10$, $F=5$, $Da=0.1$

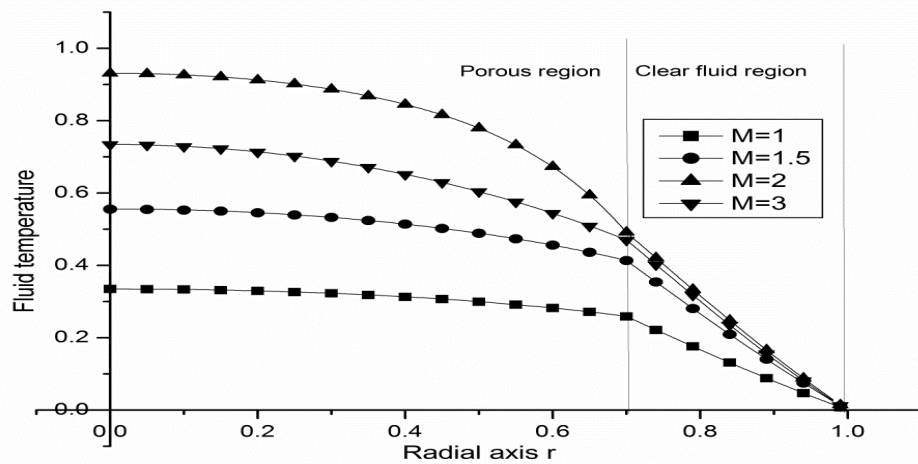


Figure 7. The effect of Hartmann number on fluid temperature at $Re=10$, $F=5$, $Da=0.01$, $G=-10$, $Br=0.01$

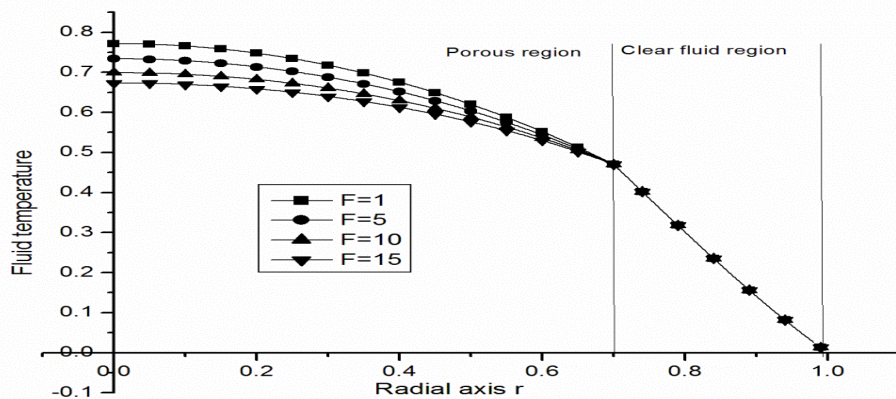


Figure 9. The effect of Forchheimer number on fluid temperature at $M=3$, $Re=10$, $Da=0.1$, $G=-10$, $Br=0.01$

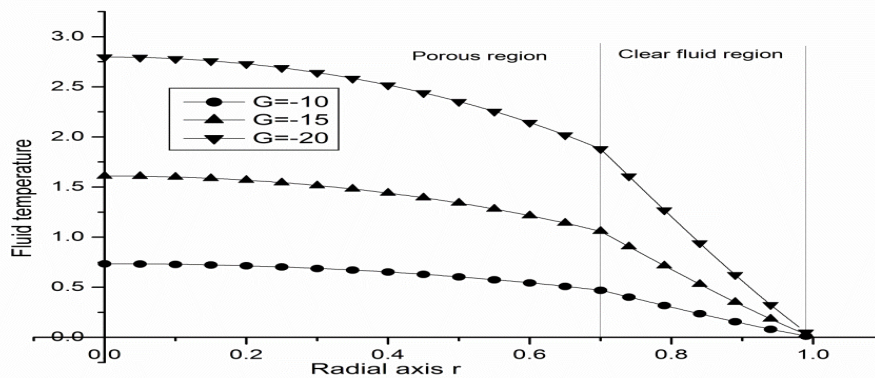


Figure 11. The effect of pressure gradient on fluid temperature at $M=3$, $Re=10$, $F=5$, $Da=0.01$, $Br=0.01$

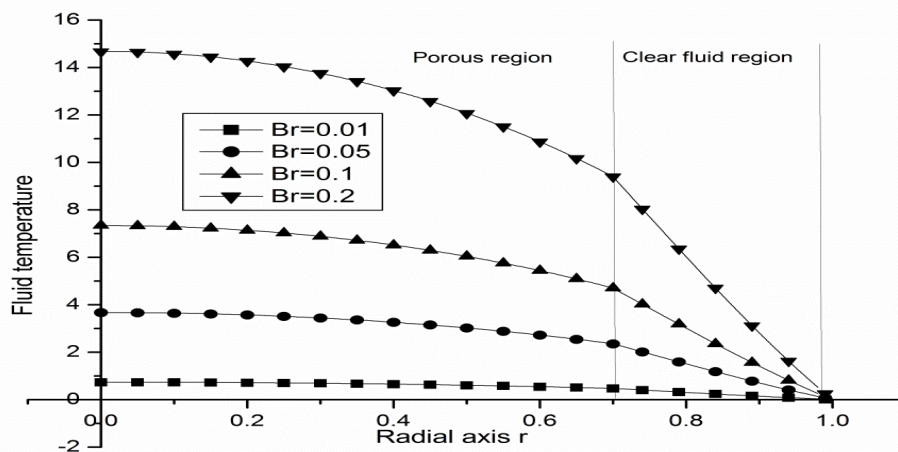


Figure 12. The effect of Brinkman number on fluid temperature at $M=3$, $Re=10$, $F=5$, $Da=0.01$, $G=-10$

REFERENCES

1. Abbas, Z., Majeed, A., Javed, T. (2013) Thermal radiation effects on MHD flow over a stretching cylinder in a porous medium.
2. Aldoss, T. K. (2014) MHD mixed convection flow about a vertical cylinder embedded in a porous medium is considered using non-Darcian model with variable heat transfer boundary. *International Communications in Heat and Mass Transfer* Vol.23 (4) pp.517-530.
3. Biazar, J., Elslami, M. (2010) Differential transform method for quadratic Riccati Differential equation. *International Journal of Nonlinear Science*, Vol.9(4) pp. 444-447.
4. Chamkha, A.J. (2011) Heat and Mass Transfer from MHD Flow over a Moving Permeable Cylinder with Heat Generation or Absorption and Chemical Reaction. *Communications in Numerical Analysis* Vol. 2011, doi 10.5899/2011/cna-00109.
5. Farshid, M. (2011) Differential transform method for solving linear and non-linear systems of ordinary differential equations. *Applied Mathematics Sciences*, Vol.5 (70), pp.3465-3472.
6. Javed, Ali (2012) One dimensional differential transform method for higher order boundary value problems in finite domain. *Int.J.Contemp.Math.Sciences*, Vol.2012(6) pp.263-272
7. Loganathan, P., Kannan, M., Ganesan, P. (2011) MHD effects on free convective flow over moving semi-infinite vertical cylinder with temperature oscillation. *Applied Mathematics & Mechanics*, Vol. 32(11), pp 1367.
8. Nagaraju, G., Murthy, J. V. R, Sai, K. S. (2013) Steady MHD flow of micropolar fluid between two rotating cylinders with porous lining. *Acta Technica Corvinensis-Bulletin of Engineering* Vol. 3(3), pp. 115.
9. Shihhao, Y., Tsai, J. C., Leong J. C. (2014) Analytical Solution for MHD Flow of a Magnetic Fluid within a Thick Porous Annulus. *Journal of Applied Mathematics* Vol. 2014, Article ID 931732, 10 pages.
10. Suneetha, S., Bhasker, R. N. (2014) Radiation and mass transfer effects on MHD free convection flow past a moving vertical cylinder in a porous medium.
11. Yadav, R. S., Sharma, P. R. (2014) Effects of Porous Medium on MHD Fluid Flow along a Stretching Cylinder. *Annals of Pure and Applied Mathematics* Vol. 6(1), pp. 104-113.
12. Ziya, U., Manoj K. (2011) Mhd Heat and Mass Transfer Free Convection Flow Near the Lower Stagnation Point of an Isothermal Cylinder Imbedded in Porous Domain with the Presence of Radiation. *Jordan Journal of Mechanical and Industrial Engineering*, Vol. 5(2) pp. 133-138.